

as the mole fraction of benzoate in the micelle approaches zero, at low ionic strength, the ratio of the concentration of benzoate in the retentate to that in the permeate will approach tremendously large values.

Acknowledgment. Financial support for this work was provided by the Office of Basic Energy Sciences of the Department of

Energy, Grant No. DE-FG01-87FE61146, and the National Science Foundation, Grant CHE 8701887. F.Z.M. expresses her appreciation for the award of a Peace Fellowship from the Egyptian Ministry of Higher Education, supported by the U.S. Agency for International Development.

Registry No. CPC, 123-03-5; sodium benzoate, 532-32-1.

Observation of Novel Photochemistry in the Multiphoton Ionization of $\text{Mo}(\text{CO})_6$ van der Waals Clusters

William R. Peifer and James F. Garvey*

Department of Chemistry, State University of New York at Buffalo, Buffalo, New York 14214

(Received: January 31, 1989)

van der Waals clusters of $\text{Mo}(\text{CO})_6$ generated in the free-jet expansion of a pulsed beam of seeded helium are subjected to multiphoton ionization and the product ions analyzed by quadrupole mass spectrometry. Oxomolybdenum and dioxomolybdenum ions are observed to be produced with high efficiency. This behavior is in striking contrast to that of metal carbonyl monomers and covalently bound cluster carbonyls, which under complete ligand loss prior to ionization. The observed photochemistry is ascribed to reactions between a photoproduct molybdenum atom and the ligands of neighboring $\text{Mo}(\text{CO})_6$ "solvent" molecules within the van der Waals cluster.

Introduction

The study of transition-metal clusters in the gas phase has experienced tremendous growth over the past decade.¹ The development of pulsed laser ablation/molecular beam sources² has made possible the study of clusters of even the most refractory of transition metals. These clusters are of fundamental significance in our understanding of metal-metal and metal-ligand bonding interactions, and they serve as model systems for the study of catalysis and surface phenomena. Studies of the effects of cluster size and structure on reactivity provide us the necessary experimental database with which to test and refine our theories concerning the chemistry and physics of bulk metals.

Reactivities of the atomic ions of the first-row transition metals in the activation of H-H bonds³⁻⁵ and C-H bonds⁶⁻⁸ have been systematically studied as functions of translational and electronic energy. Reactivity in these cases can be rationalized in terms of qualitative molecular orbital arguments and spin conservation. By contrast, dimer ions of some first- and second-row transition metals exhibit reactivities (or lack thereof) toward saturated hydrocarbons which markedly differ from those of the atomic ions.⁹⁻¹³ Furthermore, chemisorption¹⁴⁻¹⁶ and dehydrogenation^{17,18}

reactions of Nb, Co, and Fe clusters are observed to be sensitive to both the size of the cluster and the identity of the metal. The rationalization of these trends in reactivity in terms of metal-metal bonding awaits a more comprehensive theoretical understanding of the electronic structure of these larger clusters.

One might ask how trends in the reactivity of small clusters are modulated in the transition from *bare* metal clusters to *ligated* clusters (i.e., multinuclear cluster coordination compounds). Of particular importance are the large class of transition-metal carbonyl compounds. These compounds are inherently interesting because of the variety exhibited in the types of bonding between carbonyl ligands and metals.¹⁹ In addition, many coordinatively unsaturated metal carbonyl species are thought to play an important role in catalysis.²⁰ Coordinatively unsaturated metal carbonyls may be efficiently generated via photolysis of their saturated counterparts. While the condensed-phase photochemistry of metal carbonyls is dominated by the loss of a single ligand,²¹ the gas-phase photochemistry of these compounds is characterized by sequential loss of several ligands and statistical²² partitioning of excess energy among the vibrational, rotational, and translational modes of the fragments.²³⁻²⁸ Photofragmentation is even more extensive in the case of multiphoton absorption. Multiphoton ionization (MPI) of mononuclear metal carbonyls is characterized by initial multiphoton dissociation (MPD) of all ligands, yielding the bare metal atom, followed by subsequent ionization of the neutral metal.²⁹⁻³¹

(1) Gole, J. L. In *Metal Clusters*; Moskovits, M., Ed.; Wiley: New York, 1986; Chapter 6.

(2) Dietz, T. G.; Duncan, M. A.; Powers, D. E.; Smalley, R. E. *J. Chem. Phys.* **1981**, *74*, 6511.

(3) Elkind, J. L.; Armentrout, P. B. *J. Phys. Chem.* **1985**, *89*, 5626.

(4) Elkind, J. L.; Armentrout, P. B. *J. Chem. Phys.* **1986**, *84*, 4862.

(5) Elkind, J. L.; Armentrout, P. B. *J. Phys. Chem.* **1987**, *91*, 2037.

(6) Aristov, N.; Armentrout, P. B. *J. Phys. Chem.* **1987**, *91*, 6178.

(7) Georgiadis, R.; Armentrout, P. B. *J. Phys. Chem.* **1988**, *92*, 7067.

(8) Sanders, L.; Hanton, S.; Weisshaar, J. C. *J. Phys. Chem.* **1987**, *91*, 5145.

(9) Freas, R. B.; Ridge, D. P. *J. Am. Chem. Soc.* **1980**, *102*, 7129.

(10) Jacobson, D. B.; Freiser, B. S. *J. Am. Chem. Soc.* **1985**, *107*, 1581.

(11) Hettich, R. L.; Freiser, B. S. *J. Am. Chem. Soc.* **1985**, *107*, 6222.

(12) Tews, E. C.; Freiser, B. S. *J. Am. Chem. Soc.* **1987**, *109*, 4433.

(13) Huang, Y.; Freiser, B. S. *J. Am. Chem. Soc.* **1988**, *110*, 387.

(14) Geusic, M. E.; Morse, M. D.; Smalley, R. E. *J. Chem. Phys.* **1985**, *82*, 590.

(15) Whetten, R. L.; Cox, D. M.; Trevor, D. J.; Kaldor, A. *Phys. Rev. Lett.* **1985**, *54*, 1494.

(16) Richtsmeier, S.; Parks, E. K.; Liu, K.; Pobo, L. G.; Riley, S. J. *J. Chem. Phys.* **1985**, *82*, 3659.

(17) St. Pierre, R. J.; El-Sayed, M. A. *J. Phys. Chem.* **1987**, *91*, 763.

(18) St. Pierre, R. J.; Chronister, E. L.; Song, L.; El-Sayed, M. A. *J. Phys. Chem.* **1987**, *91*, 4648.

(19) Wade, K. In *Transition Metal Clusters*; Johnson, B. F. G., Ed.; Wiley: New York, 1980; Chapter 3.

(20) Whetten, R. G.; Fu, K. J.; Grant, E. R. *J. Am. Chem. Soc.* **1982**, *104*, 4270.

(21) Geoffroy, G. L.; Wrighton, M. S. *Organometallic Photochemistry*; Academic: New York, 1979.

(22) It has been recently proposed that energy disposal is rigorously described by statistical theory only in the limit of a steep exit potential surface. See: Holland, J. P.; Rosenfeld, R. N. *J. Chem. Phys.* **1988**, *89*, 7217.

(23) Nathanson, G.; Gitlin, B.; Rosan, A. M.; Yardley, J. T. *J. Chem. Phys.* **1981**, *74*, 361.

(24) Ouderkirk, A. J.; Weitz, E. J. *J. Chem. Phys.* **1983**, *79*, 1089.

(25) Seder, T. A.; Ouderkirk, A. J.; Weitz, E. J. *J. Chem. Phys.* **1986**, *85*, 1977.

(26) Fletcher, T. R.; Rosenfeld, R. N. *J. Am. Chem. Soc.* **1985**, *107*, 2203.

(27) Waller, I. M.; Davis, H. F.; Hepburn, J. W. *J. Phys. Chem.* **1987**, *91*, 506.

(28) Waller, I. M.; Hepburn, J. W. *J. Chem. Phys.* **1988**, *88*, 6658.

One might expect that MPD/MPI of the multinuclear metal cluster carbonyls would be an efficient general route to the gas-phase synthesis of specific sizes (or at least narrow size distributions) of bare metal clusters and cluster ions having well-defined internal energies. In fact, the MPD/MPI of the cluster carbonyls $\text{Mn}_2(\text{CO})_{10}$,³² $\text{Fe}_3(\text{CO})_{12}$,³³ and $\text{Co}_4(\text{CO})_{12}$ ³⁴ proceeds via complete ligand loss, followed by ionization of the nascent metal cluster (and subsequent dissociation of this cluster ion to smaller ionic fragments). However, the generality of this route to metal cluster synthesis is severely compromised by the fact that the larger cluster carbonyls have diminishingly small vapor pressures and are thermally labile.

Metal carbonyl clusters of high nuclearity may be easily formed in the gas phase through the free-jet expansion of pulsed helium beams seeded with the relatively volatile mononuclear metal carbonyls. While MPI of jet-cooled metal carbonyl monomers has been well-studied,²⁹ the multiphoton photophysics of van der Waals complexes of such metal carbonyls has not been so thoroughly investigated. $\text{Fe}(\text{CO})_5$ van der Waals complexes are known to undergo multiphoton dissociation with complete ligand loss, forming bare Fe clusters which subsequently ionize to give fragments with as many as 30 atoms.³⁵ The threshold wavelength for this multiphoton process lies somewhere between 266 and 193 nm. Novel intracuster photochemistry has been observed in the MPD/MPI of mixed van der Waals complexes containing $\text{Fe}(\text{CO})_5$ and either O_2 or CO_2 .³⁶ The appearance of oxidized Fe cluster ions, Fe_nO^+ and Fe_nO_2^+ , subsequent to MPI of these metal carbonyl heteroclusters, is attributed to a bimolecular reaction that occurs prior to ionization. Photoinduced intracuster reactivity of this type has only been observed in a limited number of heterocluster systems.³⁷⁻⁴¹

We would like to develop a more comprehensive understanding of the photophysics of metal carbonyl van der Waals complexes as well as the influence of d-orbital occupancy on intracuster photochemistry. Toward that end, we have recently initiated a series of experiments to probe the multiphoton dissociation and ionization dynamics of several metal carbonyl systems. We report herein our observation of novel intracuster photochemistry in the $\text{Mo}(\text{CO})_6$ system.

Experimental Section

In these experiments, $\text{Mo}(\text{CO})_6$ van der Waals clusters are generated in the free-jet expansion of a pulsed helium beam and subsequently photoionized by the focused output of a KrF excimer laser. Photoions are detected by a quadrupole mass spectrometer. The experimental apparatus used in these studies can be broken down into five component parts: a vacuum chamber, a pulsed molecular beam valve, the excimer laser (with ancillary optics and timing electronics), the quadrupole mass spectrometer, and, lastly, the signal acquisition electronics. The apparatus is shown schematically in Figure 1.

The vacuum chamber was custom-fabricated from 304 stainless steel and was pumped by a liquid nitrogen baffled 4-in. oil diffusion pump (Edwards E04) backed by a 23-cfm two-stage rotary pump (Edwards ED660). Attached to the chamber was a 2.75-in.

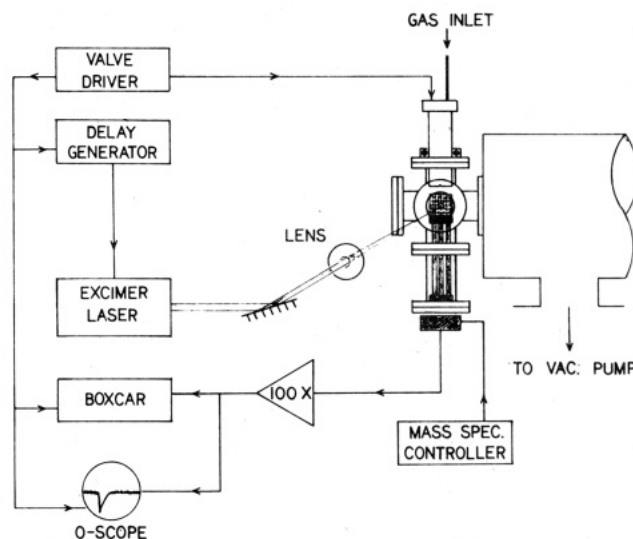


Figure 1. Experimental apparatus, shown schematically.

flanged six-way cross which was used to properly orient the pulsed valve and quadrupole mass analyzer with respect to the ionizing laser beam (vide infra). Base pressure in the vacuum chamber could be held to below 10^{-7} Torr with no gas load on the system, as measured by a Bayard-Alpert ionization gauge tube. During pulsed valve operation, the maximum chamber pressure was typically $(3-4) \times 10^{-6}$ Torr, and instantaneous pressures in the ion source did not exceed 3×10^{-5} Torr.

The pulsed molecular beam valve was a Newport BV-100 double-solenoid pulsed valve equipped with a 0.5-mm, 30° conical orifice. The quadrupole mass spectrometer was a 2.75-in. flange-mounted Dycor residual gas analyzer with an electron impact ion source and a low-gain (ca. 1000 \times) electron multiplier. This analyzer has a mass range of 1–200 amu and was operated at better than 0.5-amu resolution. The analyzer was mounted in such a manner that the ion source was situated in the center of the six-way cross. Apertures of 0.25-in. diameter were cut in the two concentric annular grids of the ion source to allow a delayed pulse of focused UV output from the ionizing laser (Lambda Physik EMG150E) unobstructed passage through the center of the source, perpendicular to the ion–optic axis (z axis). The pulsed valve was mounted in the six-way cross opposite the analyzer, about 2 in. away from the ion source, so that the molecular beam axis was coincident with the z axis of the analyzer. Although this collinear configuration leads to somewhat higher instantaneous pressures in the ion source than for the case of a perpendicular configuration, we find experimentally that a collinear configuration with this particular ion source gives a distribution of clusters peaked at larger cluster sizes (as determined, for example, by detection of photoionized methanol clusters) than does a perpendicular configuration. By monitoring cluster ion intensity as a function of the delay time between the molecular beam pulse and the photoionization laser pulse, it was determined that these ions truly result from ionization of clusters formed within the free-jet expansion, rather than from associative bimolecular ion–molecule collisions between monomeric photoions and background gas.

In our pulsed beam/photoionization experiments reported here, $\text{Mo}(\text{CO})_6$ (98%, Aldrich) is purified by several freeze–pump–thaw cycles at 77 K and seeded at its room-temperature vapor pressure (ca. 0.3 Torr) into 1.3 atm of He. This mixture is pulsed from the ca. 5-cm³ stagnation chamber of the molecular beam valve at a frequency of 1 Hz. At this rate, the chamber is able to pump back down to its base pressure between gas pulses. We have previously determined that the duration of a gas pulse delivered by this valve under similar operating conditions of solenoid driving current and repetition rate is about 100- μ s fwhm. The synchronization signal from the valve driver is used to trigger the timing circuit of a variable delay generator. After a suitable delay (typically ca. 350 μ s), this circuit sends a 15-V trigger to the

(29) Duncan, M. A.; Dietz, T. G.; Smalley, R. E. *Chem. Phys.* **1979**, *44*, 415.

(30) Gerrity, D. P.; Rothberg, L. J.; Vaida, V. *Chem. Phys. Lett.* **1980**, *74*, 1.

(31) Engelking, P. C. *Chem. Phys. Lett.* **1980**, *74*, 207.

(32) Leopold, D. G.; Vaida, V. *J. Am. Chem. Soc.* **1984**, *106*, 3720.

(33) Leutwyler, S.; Even, U. *Chem. Phys. Lett.* **1981**, *84*, 188.

(34) Hollingsworth, W. E.; Vaida, V. *J. Phys. Chem.* **1986**, *90*, 1235.

(35) Duncan, M. A.; Dietz, T. G.; Smalley, R. E. *J. Am. Chem. Soc.* **1981**, *103*, 5245.

(36) Wheeler, R. G.; Duncan, M. A. *J. Phys. Chem.* **1986**, *90*, 3876.

(37) Sivakumar, N.; Burak, I.; Cheung, W. Y.; Houston, P. L.; Hepburn, J. W. *J. Phys. Chem.* **1985**, *89*, 3609.

(38) Jouvet, C.; Soep, B. *Chem. Phys. Lett.* **1983**, *96*, 426.

(39) Breckenridge, W. H.; Jouvet, C.; Soep, B. *J. Chem. Phys.* **1986**, *84*, 1443.

(40) Radhakrishnan, G.; Buelow, S.; Wittig, C. *J. Chem. Phys.* **1986**, *84*, 727.

(41) Knee, J. L.; Otis, C. E.; Johnson, P. M. *J. Phys. Chem.* **1982**, *86*, 4467.

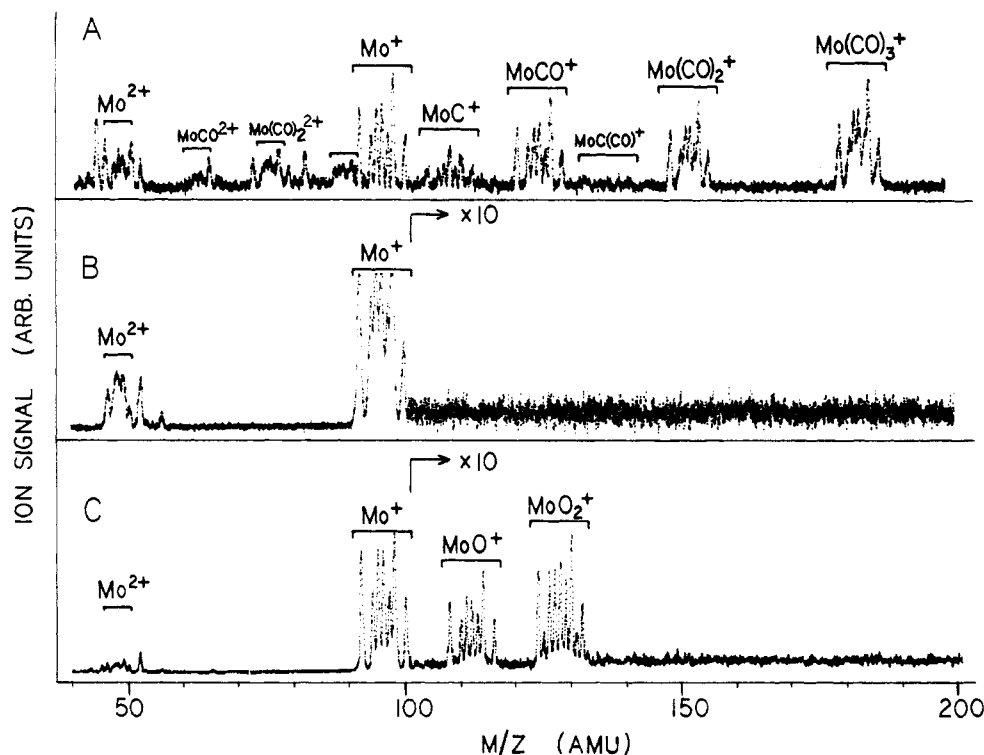


Figure 2. Mass spectra of Mo(CO)_6 , 40–200 amu. Ion signals for the three spectra are in arbitrary units and are not normalized with respect to each other. Signals at 52 and 56 amu are due to trace impurities of Cr and Fe. (A) Mo(CO)_6 van der Waals clusters; electron impact ionization. The label for the sequence of peaks corresponding to Mo(CO)_3^{2+} (88–92 amu) has been omitted for clarity. (B) Mo(CO)_6 monomer; multiphoton ionization. (C) Mo(CO)_6 van der Waals clusters; multiphoton ionization.

photoionization laser. The laser then fires a 20-ns duration laser pulse of wavelength 248 nm. The beam is reflected by several steering mirrors and focused by a fused silica lens (50-mm diameter, 250-mm focal length) to a ca. 50- μm -diameter image within the interior of the ion source of the mass spectrometer. This focused pulse is spatially and temporally coincident with the leading edge of the molecular beam pulse. Ions formed are detected by slowly scanning the mass acceptance of the quadrupole filter while monitoring the output current of the multiplier. Output from the multiplier is converted to a voltage, amplified 100 \times by a fast amplifier, and averaged with background subtraction by a boxcar averager (EG&G Princeton Applied Research Model 4420). Typical pulsed beam mass spectra are collected and averaged over 2500 laser shots, representing a mass range of 100 amu.

The dependence of a given mass-selected ion signal on laser intensity could be determined by setting the mass filter to pass ions of only a single mass-to-charge ratio and then recording the average ion signal over a set of several laser pulse energies. Typically, the ion signal at a given pulse energy was averaged over about 200 laser shots. Output from the electron multiplier was also collected while the beam was blocked to ensure that the detector dark count rate was low and that there was no electrical drift in the base line. Laser pulse energy could be varied from 6 to 210 mJ (as measured at the laser head with a thermocouple power meter) by a combination of three different methods: use of neutral density filters to partially attenuate the beam, operation of the high-voltage discharge at reduced charging voltage, and operation of the injection-locked dual cavity excimer with an inert gas fill in the amplifier cavity.

Electron impact mass spectra of Mo(CO)_6 clusters were collected by use of a 70-eV continuous electron source operated at an emission current of 1 mA in place of the pulsed 248-nm photoionization laser. In addition, electron impact and multiphoton ionization mass spectra of the unclustered Mo(CO)_6 monomer were collected by admitting metal carbonyl vapor through an effusive inlet into the vacuum chamber. The quadrupole analyzer was calibrated for sensitivity and mass scale linearity against perfluorotributylamine, admitted through the

effusive inlet, and ionized by electron impact.

Results and Discussion

The mass spectra of Mo(CO)_6 monomer and clusters, acquired through different modes of sample ionization, are shown in Figure 2a–c. The electron impact spectrum for metal carbonyl clusters, shown in Figure 2A, is virtually identical with that observed for the monomer. The fragmentation pattern is typical of that expected for initial formation of a large (possibly parent) ion with excess internal energy, followed by prompt statistical dissociation into an ensemble of daughter fragments. Because the mass range of the quadrupole analyzer used in these studies is limited, it is not possible to observe ions corresponding to solvated fragments. The MPI mass spectrum of the monomeric metal carbonyl vapor is shown in Figure 2B and displays, as expected, complete domination of the mass spectrum by the ionized metal. The MPI mass spectrum of metal carbonyl clusters is shown in Figure 2C, and even cursory observation reveals striking features. First, the spectrum shows no evidence of bare metal cluster ions, as observed in the MPI mass spectra of the covalently bound metal cluster carbonyls.^{32–34} Second, complete domination of the spectrum by the metal ion signal does *not* occur, contrasting sharply with the observed behavior of the monomer. Rather, species corresponding to oxo- and dioxomolybdenum ions appear. Third, and perhaps most striking of all, is that the production of an oxometal species via an intracluster, bimolecular mechanism implies scission of a carbonyl C–O bond at a rate that must necessarily be competitive with that of further multiphoton up-pumping. This up-pumping rate is expected to be quite fast in the regime of the high power densities encountered in the use of tightly focused excimer lasers.

Several questions now arise. First, is the observed fragmentation behavior in the MPI mass spectrum of Mo(CO)_6 clusters a manifestation of some novel intracluster metal–ligand reactivity, or is it simply the result of some experimental artifact? Second, if some novel metal–ligand reactivity is occurring within the cluster, is it an interaction between a ligand and a neutral metal photofragment or between a ligand and a metal photoion? Third, can this reactivity be explained by analogy with known metal–ligand interactions (e.g., bonding and structure in model com-

pounds, surface chemisorption phenomena, gas-phase metal ion reactivities, etc.) or rationalized, perhaps, in terms of a qualitative molecular orbital picture? Finally, within the confines of our answers to the third question, can we make any generalizations about the role of d-orbital electronic effects (occupancy number, spin, etc.) in the observed reactivity and subsequently predict trends in reactivity as a function of d-orbital participation?

We first address the question of experimental artifacts. One source of artifact is that some oxygen-containing impurity might be present in the solid metal carbonyl sample (or the small stagnation volume of the pulsed valve) which could react with photoproducted Mo atoms or ions, eventually yielding an oxomolybdenum ion. We observe no evidence of *detectable* levels (by electron impact mass spectroscopy) of such impurities within either the metal carbonyl sample or the stagnation volume of the valve; however, water, methanol, and (to a lesser extent) molecular oxygen are detected at very low levels within the vacuum chamber itself. (These species are observed to chemisorb on neutral aluminum clusters.⁴²) While we cannot completely discount the possibility that these compounds are present as impurities in the sample or valve at levels below the detection limit of our mass spectrometer, we feel that such low levels of impurities would not lead to a significant population of "impure" van der Waals clusters within the pulsed molecular beam. The observation of ^{18}O oxomolybdenum ions in the MPI mass spectrum of ^{18}O -labeled metal carbonyl clusters would allow one to unambiguously eliminate this first source of artifact.

A second source of artifact arises from the possibility that metal carbonyl vapor could be scattered from the molecular beam pulse and persist in the ion source for some time interval after the end of the pulse. Photoproducted Mo atoms or ions might react with this scattered background gas to produce oxomolybdenum ions (which would be detected immediately) or neutral metal oxides (which, if they persisted until the next laser pulse, might be subsequently photoionized and detected). We discount this possibility for the following reasons. If metal atoms (or ions) were reacting with background gas to form oxomolybdenum ions, one would expect to see these ions even if the photoionization laser was timed to fire after the end of the molecular beam pulse. However, these ions are only seen for a very narrow distribution of laser delay times which coincide with the period during which the pulsed valve is open. Furthermore, the signal from product ions resulting from reaction of Mo^+ with background gas would be expected to increase as the yield of Mo^+ increases. This behavior is not observed in the laser intensity dependence of the oxomolybdenum ions.

A third source of artifact is the possibility that photoproducted Mo atoms or ions might react with oxygen-containing impurities present at low levels within the vacuum chamber, leading to spurious production of oxomolybdenum ions. If this were the case, one would expect to see these spurious ions in the MPI mass spectrum of the $\text{Mo}(\text{CO})_6$ vapor from the effusive source as well as from the pulsed beam source. Based on the fact that such ions are not seen in the case of $\text{Mo}(\text{CO})_6$ from the effusive source, as well as on arguments based on temporal behavior and intensity dependence of the oxomolybdenum ions as discussed in the preceding paragraph, this third source of artifact is discounted.

Since we have a large body of evidence to suggest that the oxomolybdenum ions do *not* arise out of an experimental artifact, but rather from some photochemically induced intracuster process, we now must consider whether they arise out of interactions of the carbonyl ligands with a molybdenum photoion or, alternatively, a neutral molybdenum atom. In order to address this question, we consider the laser intensity dependence of the signals for various ionic species detected in the MPI mass spectrum of the $\text{Mo}(\text{CO})_6$ clusters. Figure 3 shows a plot of the log of ion signal vs the log of the laser pulse energy for the ions $^{98}\text{Mo}^+$, $^{98}\text{MoO}^+$, and $^{98}\text{MoO}_2^+$. While the yield of Mo^+ is observed to depend on the square root of laser intensity, yields for both of the oxomolybdenum

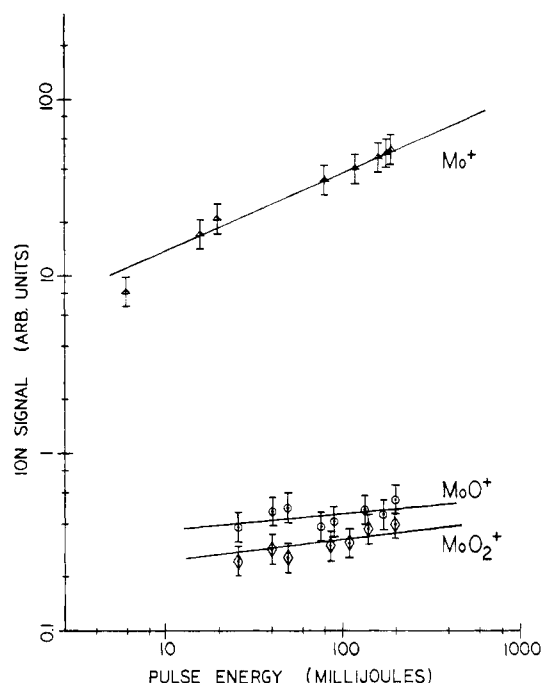


Figure 3. Plot of log (ion signal) vs log (laser pulse energy). The experimentally observed ion signal is proportional to the laser intensity raised to the power n . From the log-log plots, the values of n for $^{98}\text{Mo}^+$, $^{98}\text{MoO}^+$, and $^{98}\text{MoO}_2^+$ are found to be 0.5, 0.09, and 0.1, respectively.

ionic species are found to be nearly independent of laser intensity across the range of pulse energies investigated here. Interpretation of this intensity dependence data must be done with extreme care, since the observed intensity dependence under conditions of very high power density is subject to spectroscopic⁴³ and geometric⁴⁴ effects which do not reflect the inherent photophysics of the multiphonon process. It would not be prudent, then, to draw detailed inferences about specific dynamical processes leading to formation of the three ions considered here. We *can* say, however, that the mechanism leading to production of Mo^+ remains sensitive to laser intensity over the range of intensities investigated, while the mechanism leading to production of the oxomolybdenum ions is nearly saturated within this range of intensities. Therefore, we conclude that we are probably observing two *distinct* processes, one leading to a molybdenum ion and the other leading to oxomolybdenum ions, and that the oxomolybdenum ions most likely do *not* arise from reactions of the nascent molybdenum photoion.

If the oxomolybdenum ions arise from reactions of the neutral molybdenum atom, then the mass-selected resonance-enhanced MPI (REMPI) spectrum, observed by monitoring MoO^+ or MoO_2^+ yield vs photoionization wavelength, should show resonant features assignable to atomic molybdenum transitions. This would be an excellent means by which to assess the importance of excited states of molybdenum in the observed photochemistry, since REMPI features assignable to transitions from ground-state molybdenum atoms would appear at different wavelengths than, and hence be distinguishable from, features assignable to transitions from excited-state atoms.^{45,46}

Although it is not possible, based on the results of our present experiments, to draw definitive conclusions regarding the geometry of the metal-ligand interactions leading to the observed photoions, we can certainly gain insights concerning likely candidates for transition-state structures by analogy with model systems. We now consider two very different kinds of models which involve attachment of one end of a carbonyl ligand to one metal atom with simultaneous attachment of the other end to a different metal atom: first, novel compounds in which carbonyl ligands act as

(42) Cox, D. M.; Trevor, D. J.; Whetten, R. L.; Kaldor, A. *J. Phys. Chem.* **1988**, *92*, 421.

(43) Gontier, Y.; Trahin, M. *Phys. Rev. A* **1973**, *7*, 1899.

(44) Cervenán, M. R.; Isenor, N. R. *Opt. Commun.* **1975**, *13*, 175.

(45) Nagano, Y.; Achiba, Y.; Kimura, K. *J. Phys. Chem.* **1986**, *90*, 615.

(46) Nagano, Y.; Achiba, Y.; Kimura, K. *J. Phys. Chem.* **1986**, *90*, 1288.

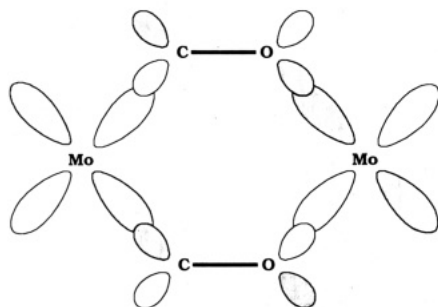


Figure 4. Postulated transition structure in the multiphoton dissociation/ionization of a Mo(CO)_6 van der Waals cluster, showing overlap of the d_{xy} atomic orbitals of two Mo atoms with the π^* molecular orbitals of two bridging carbonyl ligands. The metal d_{2z} atomic orbitals and the carbonyl π_{2z} molecular orbitals are normal to the plane of the six-membered ring.

four-electron donors; and second, metal surfaces to which carbon monoxide is chemisorbed.

Four-electron, doubly bridging coordination of carbonyl ligands is rarely seen in isolable organotransition-metal compounds, although it may be important among coordinatively unsaturated reaction intermediates.¹⁹ This bridging may be unsymmetrical, in which the ligand binds to one metal through a terminal bond while binding to the other metal in a dihapto fashion through a $d-\pi^*$ interaction. An example of this is found in the dinuclear manganese complex $\text{Mn}_2(\text{CO})_5(\text{Ph}_2\text{PCH}_2\text{PPh}_2)_2$.⁴⁷ Bridging may also be symmetrical, involving donation of the lone-pair electrons of a terminally bound carbonyl to a second metal center. This can be regarded as a Lewis acid-base interaction between the (basic) oxygen atom and a metal atom with Lewis acid character.⁴⁸ This type of bonding is known to occur in the complex $[\text{CpMo}(\text{CO})_3]_2\text{Mg}(\text{Py})_4$.⁴⁹ Analogous complexes of the cyclopentadienyl group VI tricarbonyls can also form in which the Lewis acid is Mn instead of Mg.⁵⁰ An example of dihapto bridging involving the isoelectronic dinitrogen ligand is also known in which two tungsten atoms are symmetrically bridged.⁵¹

Let us consider metal-carbonyl interactions in a different sense, that is, the chemisorption of CO on metal surfaces. This phenomenon has been examined both experimentally and theoretically. Under conditions of low coverage, CO is observed to chemisorb on Cr(110) in a "lying-down" fashion, with the CO interatomic axis parallel to the crystal surface.^{52,53} The CO stretching frequencies and bond order are reduced with respect to perpendicularly chemisorbed CO. These results have been corroborated theoretically.⁵⁴ The stretching frequencies for CO chemisorbed on Mo(100) at low coverage are unusually low,⁵⁵ only 1065 and 1235 cm^{-1} . Chemisorption of CO on Pt(111) has been examined theoretically in model calculations on a Pt_{22} cluster doped with a single metal atom or metal oxide molecule.⁵⁶ A reduced bond

order and stretching frequency and a nonperpendicular orientation of chemisorption are predicted.

What can we infer about structures of transition states in the photochemistry of metal carbonyl van der Waals complexes, based on analogies drawn from surface science and inorganic synthetic chemistry that we considered above? It seems not unreasonable that the photochemistry we are observing proceeds through the intermediacy of transition states involving doubly bridging, dihapto carbonyl ligands. We speculate, strictly on the basis of orbital symmetry considerations, that the nascent metal photoproduct may interact with a neighboring metal carbonyl "solvent molecule" via two such bridging carbonyls through back-donation of metal d_{xy} electron density to the empty π^* MO's of the carbonyl ligands, as suggested in Figure 4. This model is consistent with the fact that we observe efficient production of oxo- and dioxomolybdenum ions yet fail to detect oxides of higher stoichiometry. This bonding scheme is somewhat analogous to the two-electron, three-center bonding in B_2H_6 . Such a structure would be *destabilized* by electron density in the π_y MO's of the carbonyl ligands, but would be *stabilized* in a Hückel sense, assuming a planar structure, if the total occupancy number of the metal d_{2z} orbitals was 2 (four p_z electrons from the carbonyls plus two d_{2z} electrons from the metals). Structures similar to the one we propose here have been invoked by Russell and co-workers to explain observed trends in the ion-molecule reactions of coordinatively unsaturated metal carbonyls.⁵⁷⁻⁶⁰ We can test our structural hypotheses by attempting to observe transient neutral metal carbonyl species using the technique of MPD-electron impact mass spectroscopy.⁶¹ We are currently extending these studies to other metal carbonyl systems having different d-orbital occupancy numbers to assess the level of d-orbital participation in the observed chemistry and to test our structural hypotheses.

Conclusions

We have examined the 248-nm multiphoton ionization dynamics of Mo(CO)_6 van der Waals clusters generated in pulsed supersonic molecular beams. We have found compelling evidence of striking photochemical behavior, heretofore unobserved in the multiphoton ionization of transition-metal carbonyls, which we attribute to a reaction between the nascent atomic metal photoproduct and one or more ligands of an adjacent metal carbonyl "solvent molecule". This observation may have important implications in our fundamental understanding of heterogeneous catalysis and chemisorption processes on metal surfaces. We are currently extending these experiments to other transition-metal coordination compounds in order to structurally characterize reactive intermediates and investigate the role of d-orbital participation in the observed photochemistry.

Acknowledgment. We gratefully acknowledge the Office of Naval Research (Contract No. N00014-88-K-0493) and the donors of the Petroleum Research Fund, administered by the American Chemical Society, for partial support of this research. We also acknowledge Newport Corp. for an equipment grant.

Registry No. Mo(CO)_6 , 13939-06-5; MoO^+ , 71252-77-2; MoO_2^+ , 19583-09-6; Mo, 7439-98-7.

(47) Commons, C. J.; Hoskins, B. F. *Aust. J. Chem.* **1975**, *28*, 1663.

(48) Shriver, D. F.; Alich, A., Sr. *Coord. Chem. Rev.* **1972**, *8*, 15.

(49) Ulmer, S. W.; Skarstad, P. M.; Burlitch, J. M.; Hughes, R. E. *J. Am. Chem. Soc.* **1973**, *95*, 4469.

(50) Blackmore, T.; Burlitch, J. M. *J. Chem. Soc., Chem. Commun.* **1973**, 405.

(51) Anderson, S. N.; Richards, R. L.; Hughes, D. L. *J. Chem. Soc., Chem. Commun.* **1982**, 1291.

(52) Shinn, N. D.; Madey, T. E. *J. Chem. Phys.* **1985**, *83*, 5928.

(53) Shinn, N. D.; Madey, T. E. *Phys. Rev. Lett.* **1984**, *53*, 2481.

(54) Mehandru, S. P.; Anderson, A. B. *Surf. Sci.* **1986**, *169*, L281.

(55) Zaera, F.; Kollin, E.; Gland, J. L. *Chem. Phys. Lett.* **1985**, *121*, 464.

(56) Anderson, A. B.; Dowd, D. Q. *J. Phys. Chem.* **1987**, *91*, 869.

(57) Fredeen, D. A.; Russell, D. H. *J. Am. Chem. Soc.* **1985**, *107*, 3762.

(58) Fredeen, D. A.; Russell, D. H. *J. Am. Chem. Soc.* **1986**, *108*, 1860.

(59) Fredeen, D. A.; Russell, D. H. *J. Am. Chem. Soc.* **1987**, *109*, 3903.

(60) Tecklenburg, Jr., R. E.; Russell, D. H. *J. Am. Chem. Soc.* **1987**, *109*, 7654.

(61) Prinslow, D. A.; Vaida, V. *J. Am. Chem. Soc.* **1987**, *109*, 5097.